J|A|C|S
ARTICLES
Published on Web 06/11/2004

Tunable Photonic Band Gap Crystals Based on a Liquid Crystal-Infiltrated Inverse Opal Structure

Shoichi Kubo,[†] Zhong-Ze Gu,[‡] Kazuyuki Takahashi,[§] Akira Fujishima,[||] Hiroshi Segawa,[†,⊥] and Osamu Sato*,[||]

Contribution from the Department of Applied Chemistry, School of Engineering, The University of Tokyo, 3-8-1 Komaba, Meguro-ku, Tokyo 153-8902, Japan, National Laboratory of Molecular and Biomolecular Electronics, Southeast University, Nanjing 210096, China, Institute for Molecular Science, 38 Nishigo-Naka, Myodaiji, Okazaki 444-8585, Japan, Kanagawa Academy of Science and Technology, KSP Building, East 412, 3-2-1 Sakado, Takatsu-ku, Kawasaki-shi, Kanagawa 213-0012, Japan, and Department of Chemistry, School of Arts and Sciences, The University of Tokyo, 3-8-1 Komaba, Meguro-ku, Tokyo 153-8902, Japan

Received January 28, 2004; E-mail: sato@photo-science.jp

Abstract: Composite materials comprised of nematic liquid crystals (LCs) and SiO_2 inverse opal films were fabricated. Their optical properties were quite different from those of inverse opal films without the LCs. The optical properties could be controlled by changing the refractive indices of the LCs, which vary with orientation, phase, and temperature. In particular, the optical properties were drastically changed by thermal or photoinduced isothermal phase transitions of the LCs. This means that the photonic band structure could be controlled, and tunable photonic crystals have been achieved, based on the inverse opal structure. The mechanism of this change was investigated by the evaluation of the effective refractive indices. As a result, it was found that the change in optical properties was derived from the orientation of the LC molecules in the voids in the inverse opal film. Furthermore, once the mechanism was understood, it was also possible to control the position of the reflection peak by changing the alignment of the LCs. Such materials have the possibility for practical use in optical devices and fundamental research systems.

Introduction

Recently, photonic band gap (PBG) crystals composed of spatially ordered dielectrics with lattice parameters comparable to the wavelength of visible light have received much attention due to their unique properties in controlling the propagation of light.[1−28] Many potential applications of photonic crystals require some capability for tuning the band structure through external stimuli.[29−50] The photonic band structure mainly

[†] School of Engineering, The University of Tokyo.
[‡] Southeast University.
[§] Institute for Molecular Science.
[||] Kanagawa Academy of Science and Technology.
[⊥] School of Arts and Sciences, The University of Tokyo.

(1) Yablonovitch, E. *Phys. Rev. Lett.* **1987**, *58*, 2059.
(2) John, S. *Phys. Rev. Lett.* **1987**, *58*, 2486.
(3) Joannopoulos, J. D.; Meade, R. D.; Winn, J. N. *Photonic Crystals: Molding the Flow of Light*; Princeton University Press: Princeton, NJ, 1995.
(4) Kim, B. G.; Parikh, K. S.; Ussery, G.; Zakhidov, A.; Baughman, R. H.; Yablonobitch, E.; Dunn, B. S. *Appl. Phys. Lett.* **2002**, *81*, 4440.
(5) Joannopoulos, J. D.; Villeneuve, P. R.; Fan, S. *Nature* **1997**, *386*, 143.
(6) Tarhan, İ. İ.; Watson, G. H. *Phys. Rev. Lett.* **1996**, *76*, 315.
(7) Park, S. H.; Xia, Y. *Langmuir* **1999**, *15*, 266.
(8) Xia, Y.; Gates, B.; Yin, Y.; Lu, Y. *Adv. Mater.* **2000**, *12*, 693.
(9) Jiang, P.; Bertone, J. F.; Hwang, K. S.; Colvin, V. L. *Chem. Mater.* **1999**, *11*, 2132.
(10) Jiang, P.; Hwang, K. S.; Mittleman, D. M.; Bertone, J. F.; Colvin, V. L. *J. Am. Chem. Soc.* **1999**, *121*, 11630.
(11) Míguez, H.; Meseguer, F.; López, C.; Mifsud, A.; Moya, J. S.; Vázquez, L. *Langmuir* **1997**, *13*, 6009.
(12) Míguez, H.; Meseguer, F.; López, C.; López-Tejeira, F.; Sánchez-Dehesa, J. *Adv. Mater.* **2001**, *13*, 393.
(13) Bertone, J. F.; Jiang, P.; Hwang, K. S.; Mittleman, D. M.; Colvin, V. L. *Phys. Rev. Lett.* **1999**, *83*, 300.
(14) Velev, O. D.; Jede, T. A.; Lobo, R. F.; Lenhoff, A. M. *Nature* **1997**, *389*, 447.
(15) Tessier, P. M.; Velev, O. D.; Kalambur, A. T.; Rabolt, J. F.; Lenhoff, A. M.; Kaler, E. W. *J. Am. Chem. Soc.* **2000**, *122*, 9554.
(16) Velev, O. D.; Kaler, E. W. *Adv. Mater.* **2000**, *12*, 531.
(17) Blanco, A.; Chomski, E.; Grabtchak, S.; Ibisate, M.; John, S.; Leonard, S. W.; Lopez, C.; Meseguer, F.; Miguez, H.; Mondia, J. P.; Ozin, G. A.; Toader, O.; Driel, H. M. v. *Nature* **2000**, *405*, 437.
(18) García-Santamaría, F.; Ibisate, M.; Rodríguez, I.; Meseguer, F.; López, C. *Adv. Mater.* **2003**, *15*, 788.
(19) Trau, M.; Saville, D. A.; Aksay, I. A. *Science* **1996**, *272*, 706.
(20) van Blaaderen, A. *Science* **1998**, *282*, 887.
(21) Reynolds, A. L.; Cassagne, D.; Jouanin, C.; Arnold, J. M. *Synth. Met.* **2001**, *116*, 453.
(22) Romanov, S. G.; Maka, T.; Torres, C. M. S.; Müller, M.; Zentel, R. *Synth. Met.* **2001**, *116*, 475.
(23) Yoshino, K.; Lee, S. B.; Tatsuhara, S.; Kawagishi, Y.; Ozaki, M.; Zakhidov, A. A. *Appl. Phys. Lett.* **1998**, *73*, 3506.
(24) Vlasov, Y. A.; Astratov, V. N.; Karimov, O. Z.; Kaplyanskii, A. A.; Bogomolov, V. N.; Prokofiev, A. V. *Phys. Rev. B* **1997**, *55*, 13357.
(25) Marlow, F.; Dong, W. *ChemPhysChem* **2003**, *4*, 549.
(26) Gu, Z.-Z.; Meng, Q.-B.; Hayami, S.; Fujishima, A.; Sato, O. *J. Appl. Phys.* **2001**, *90*, 2042.
(27) Gu, Z.-Z.; Hayami, S.; Kubo, S.; Meng, Q.-B.; Einaga, Y.; Tryk, D. A.; Fujishima, A.; Sato, O. *J. Am. Chem. Soc.* **2001**, *123*, 175.
(28) Gu, Z.-Z.; Kubo, S.; Fujishima, A.; Sato, O. *Appl. Phys. A* **2002**, *74*, 127.
(29) Yoshino, K.; Kawagishi, Y.; Ozaki, M.; Kose, A. *Jpn. J. Appl. Phys.* **1999**, *38*, L786.
(30) Holtz, J. H.; Asher, S. A. *Nature* **1997**, *389*, 829.
(31) Weissman, J. M.; Sunkara, H. B.; Tse, A. S.; Asher, S. A. *Science* **1996**, *274*, 959.
(32) Lee, K.; Asher, S. A. *J. Am. Chem. Soc.* **2000**, *122*, 9534.
(33) Gu, Z.-Z.; Fujishima, A.; Sato, O. *J. Am. Chem. Soc.* **2000**, *122*, 12387.
(34) Reese, C. E.; Mikhonin, A. V.; Kamenjicki, M.; Tikhonov, A.; Asher, S. A. *J. Am. Chem. Soc.* **2004**, *126*, 1493.
(35) Gu, Z.-Z.; Hayami, S.; Meng, Q.-B.; Iyoda, T.; Fujishima, A.; Sato, O. *J. Am. Chem. Soc.* **2000**, *122*, 10730.
(36) Gu, Z.-Z.; Iyoda, T.; Fujishima, A.; Sato, O. *Adv. Mater.* **2001**, *13*, 1295.
(37) Zhou, J.; Sun, C. Q.; Pita, K.; Lam, Y. L.; Zhou, Y.; Ng, S. L.; Kam, C. H.; Li, L. T.; Gui, Z. L. *Appl. Phys. Lett.* **2001**, *78*, 661.

10.1021/ja0495056 CCC: $27.50

depends on the lattice constants and the refractive indices of the dielectrics. Some practical schemes have been reported that are based on the concept of changing the lattice constants. Mechanically tunable photonic crystals have been fabricated using elastic spheres, where the band can be controlled by an external mechanical force.[29] Control of the spatial structure has also been realized by taking advantage of the volume phase transition of hydrogels, where the photonic band structures have been tuned by controlling the temperature, the pH, and the ionic state.[30−32] In addition, control of the photonic band structure has also been realized by utilizing the phase transition of colloidal crystals in solution, where the stop band, which is the wavelength region where the propagation of light is forbidden, can be tuned by using light.[33] Large shifts in the optical stop band have been demonstrated by controlling the lattice constants. However, these techniques have the disadvantage that structural changes of these types occur on the order of micrometer dimensions, resulting in difficulties for practical applications. The techniques using nanogels are proposed to resolve such a problem.[34] Some methods that work by controlling the refractive indices have also been studied, in which dyes are used as a medium for changing the refractive indices.[35,36] In these systems, an appropriate photochromic dye should be chosen, depending on the position of the stop band.

It is also anticipated that the use of liquid crystals (LCs) might enable tunability in photonic crystals, because LCs can exhibit optical anisotropy. Their refractive indices can be changed by controlling the direction of the molecules or the temperature. The properties of LCs can also be changed by a transition between the liquid crystal phase and the isotropic phase, or between the different types of LC phases. A practical scheme for tuning the band structure using LCs has recently been proposed, and electrically and thermally tunable photonic band gap composites have already been reported.[40−50] However, in most cases, the changes in the optical stop band were not large, and complete switching has yet to be realized. In this paper, we will report a new type of tunable photonic crystal that can be realized by using the phase transition of LCs or by controlling their orientation. Furthermore, we will also report the mechanism of these changes in the optical properties, which are supported by an evaluation of the effective indices of LCs in the cavities of inverse opal films under temperature control.

Experimental Section

Materials. Monodispersed polystyrene spheres were purchased from Duke Scientific Corp. (USA). A colloidal solution of SiO_2 nanoparticles was purchased from Catalysis & Chemicals Industries Co., Ltd. (Japan). The nematic liquid crystal 4-pentyl-4′-cyanobiphenyl (5CB) was purchased from Merck (USA). 4-Hexyl-4′-cyanobiphenyl (6CB) and 4-heptyl-4′-cyanobiphenyl (7CB) were purchased from Tokyo Kasei Kogyo Co., Ltd. (Japan). 4-Octyl-4′-cyanobiphenyl (8CB) was purchased from Aldrich (USA). 4-Buthyl-4′-methoxyazobenzene (AzoLC) was synthesized according to the literature.[51] Briefly, this involved synthesis via a diazo-coupling reaction between 4-butylaniline and phenol, followed by alkylation with methyl iodide. Solutions of the precursors for polyimide compounds for homogeneous alignment (AL1454) and homeotropic alignment (JALS-2021-R1) were purchased from JSR Corp. (Japan).

Fabrication of Inverse Opal Films. The tunable PBG crystals were based on inverse opal films. They were fabricated by a dipping method previously developed by us,[28] as follows. Polystyrene (PS) opal films were fabricated by a vertical deposition method.[9] Glass substrates were fixed vertically into a suspension containing 0.5 vol % of monodispersed PS spheres with a diameter of 235 nm and were maintained at constant temperature and humidity of 50 °C and 30%, respectively. The PS opal films were then sintered at 80 °C for 30 min to induce a stronger contact between each of the spheres or between the spheres and the glass substrate. They were then immersed in an alcoholic colloidal solution of SiO_2 nanoparticles with a diameter of 6 nm and lifted with a constant speed of 8 μm/s. During this procedure, SiO_2 nanoparticles are infiltrated into the voids in the PS opal films, which become completely filled by capillary forces and convection fluxes driven by evaporation. Finally, the samples were calcined at 500 °C for 1 h to remove the PS spheres and to solidify the nanoparticles forming the inverse opal structure.

The structures of the inverse opal films were observed by scanning electron microscopy (SEM), which was carried out on a JEOL model JSM-5400 SEM.

Infiltration of Liquid Crystals into Inverse Opal Films. The inverse opal films that were prepared by the method described above were fixed to another piece of glass. LCs were then infiltrated into the voids in the films by using capillary forces. Note that when the LCs were infiltrated into the voids, they were heated above the phase transition temperature to put them into the isotropic phase, thereby enabling them to be introduced into the voids.

Measurement of the Optical Properties. The optical properties of the liquid crystal-infiltrated inverse opal films were evaluated using the reflection spectra from vertically incident white light. The spectra were measured by using a multichannel photodetector connected to a Y-type optical fiber with an Ocean Optics S2000 spectrometer. Temperature-controlled measurements were carried out on an HCS402 Microscope Hot and Cold Stage with an STC2000 Controller (INSTEC, USA).

Results and Discussion

Observation of the Inverse Opal Structure. Figure 1 shows SEM images of the opal structure and the inverse opal structure films. It can be confirmed that the opal structure film contains closely packed hexagonal spheres. In the image of the inverse opal film, a hexagonal structure, which is derived from the FCC opal structure, can be observed, and this shows that the opal structure was well replicated. It should be noted that the surface of the inverse opal film is open, as shown by the SEM image. Additionally, the voids are not isolated, but rather are connected with each other through air holes that are derived from the contact points of PS spheres that were used to form the opal structure. That is why the next layer can be observed under the first layer in the SEM image of the inverse opal structure.

Tuning of the Photonic Band Gap Structure. Figure 2 shows the changes in the reflection spectra of the LC (5CB)-

(38) Li, B.; Zhou, J.; Li, L.; Wang, X. J.; Liu, X. H.; Zi, J. *Appl. Phys. Lett.* **2003**, *83*, 4704.
(39) Xu, C.; Hu, X.; Li, Y.; Fu, X. L.; Zi, J. *Phys. Rev. B* **2003**, *68*, 193201.
(40) Busch, K.; John, S. *Phys. Rev. Lett.* **1999**, *83*, 967.
(41) Yoshino, K.; Satoh, S.; Shimoda, Y.; Kawagishi, Y.; Nakayama, K.; Ozaki, M. *Jpn. J. Appl. Phys.* **1999**, *38*, L961.
(42) Kang, D.; Maclennan, J. E.; Clark, N. A.; Zakhidov, A. A.; Baughman, R. H. *Phys. Rev. Lett.* **2001**, *86*, 4052.
(43) Johri, G. K.; Tiwari, A.; Johri, M.; Yoshino, K. *Jpn. J. Appl. Phys.* **2001**, *40*, 4565.
(44) Shimoda, Y.; Ozaki, M.; Yoshino, K. *Appl. Phys. Lett.* **2001**, *79*, 3627.
(45) Meng, Q.-B.; Fu, C.-H.; Hayami, S.; Gu, Z.-Z.; Sato, O.; Fujishima, A. *J. Appl. Phys.* **2001**, *89*, 5794.
(46) Ozaki, M.; Shimoda, Y.; Kasano, M.; Yoshino, K. *Adv. Mater.* **2002**, *14*, 514.
(47) Takeda, H.; Yoshino, K. *J. Appl. Phys.* **2002**, *92*, 5658.
(48) Mertens, G.; Röder, T.; Schweins, R.; Huber, K.; Kitzerow, H.-S. *Appl. Phys. Lett.* **2002**, *80*, 1885.
(49) Mach, P.; Wiltzius, P.; Megens, M.; Weitz, D. A.; Lin, K.-h.; Lubensky, T. C.; Yodh, A. G. *Phys. Rev. E* **2002**, *65*, 031720.
(50) Mach, P.; Wiltzius, P.; Megens, M.; Weitz, D. A.; Lin, K.-h.; Lubensky, T. C.; Yodh, A. G. *Europhys. Lett.* **2002**, *58*, 679.
(51) Zienkiewicz, J.; Galewski, Z. *Liq. Cryst.* **1997**, *23*, 9.

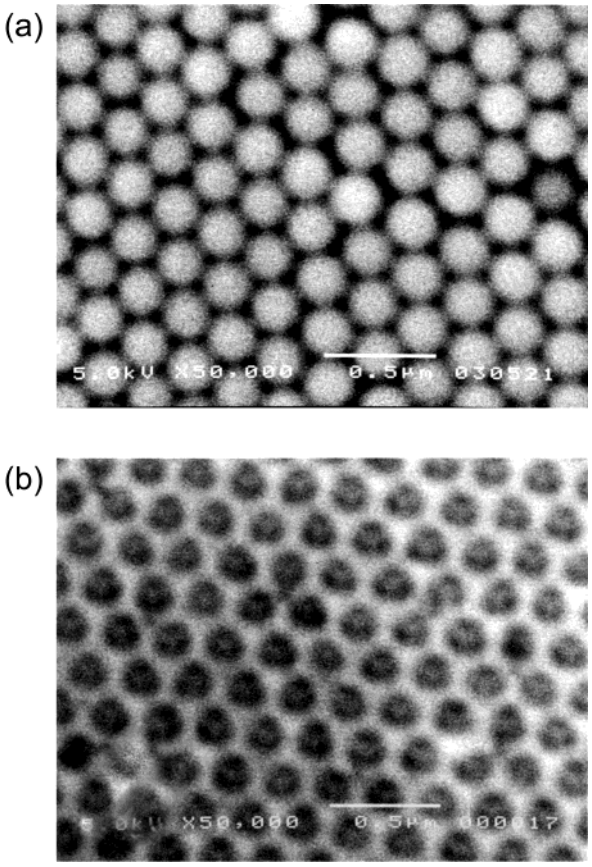

Figure 1. SEM images of polystyrene opal film (a), and SiO_2 inverse opal film (b).

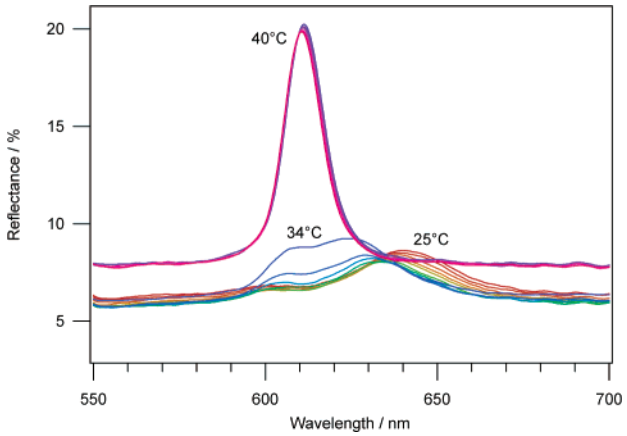

Figure 2. Reflection spectra of 5CB-infiltrated inverse opal. The spectra are plotted for temperature increments of 1 °C.

infiltrated inverse opal film with an increase in the temperature from 25 to 40 °C. In the initial state, in which the LCs are in the nematic phase, two weak peaks could be observed. The positions of the peaks shifted slowly with the gradual temperature rise, and a distinct peak at around 610 nm, which is derived from the optical stop band, appeared rapidly at the phase transition temperature. Such a change in the optical properties could also be observed visually as a change in the color of this film. Figure 3 shows photographs of the sample film before and after passing through the phase transition temperature. When the LCs are in the nematic phase, the film is white. After the phase transition into the isotropic phase, a red color could be observed, which corresponded to the peak in the reflection

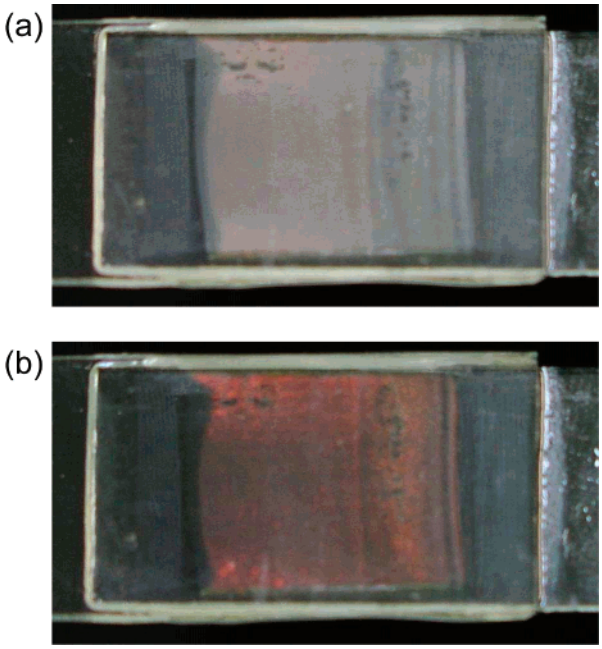

Figure 3. Photographs of sample film below phase transition temperature (a), and above phase transition temperature (b).

spectra. This result shows that switching of the optical properties can be realized due to a phase transition of the LCs, leading to thermotunable photonic crystals.

Thermal tuning of the photonic band structure has important implications, because it leads to the possibility of complete control of the optical properties. However, for practical applications, there is still the disadvantage that it is difficult to control the temperature exactly and rapidly. Additionally, it is not always desirable to change the temperature of devices. This problem can be resolved by tuning of the PBG by a photoinduced phase transition of the LCs.

As reported previously, the optical properties of LC-infiltrated inverse opal films can also be controlled by a photoinduced phase transition of the LCs.[52] Photoswitchable photonic crystals were fabricated by the infiltration of photoresponsive LCs into inverse opal films. The photoresponsive LCs used in this system are a mixture of 5CB and 4-butyl-4′-methoxyazobenzene (AzoLC) in a volume ratio of 97:3.[53,54] Light from an Hg lamp passed through a band-pass filter was used as an ultraviolet pump (λ < 365 nm, light intensity = ca. 1.5 mW/cm^2), and light from an Hg lamp passed through an interference filter was used as the visible light source ($\lambda \approx$ 450 nm, light intensity = ca. 0.75 mW/cm^2). In the initial state, only a very weak peak could be observed. The optical properties changed drastically after irradiation with the UV light. A reflection peak derived from an optical stop band at around 600 nm increased rapidly and then saturated. Following subsequent irradiation with visible light, the peak decreased rapidly and the reflection spectrum reverted completely to the original state. The origin of this change was the photoisomerization of AzoLC in the films, leading to a photoinduced phase transition of the LCs. The trans form of AzoLC shows absorption maxima at around 360 nm

(52) Kubo, S.; Gu, Z.-Z.; Takahashi, K.; Ohko, Y.; Sato, O.; Fujishima, A. *J. Am. Chem. Soc.* **2002**, *124*, 10950.
(53) Tazuke, S.; Kurihara, S.; Ikeda, T. *Chem. Lett.* **1987**, 911.
(54) Sung, J. H.; Hirano, S.; Tsutsumi, O.; Kanazawa, A.; Shiono, T.; Ikeda, T. *Chem. Mater.* **2002**, *14*, 385.

due to the $\pi-\pi^*$ transition, and at around 450 nm due to the n$-\pi^*$ transition. The excitation of the $\pi-\pi^*$ transition of *trans*-AzoLC at around 360 nm results in a transformation to *cis*-AzoLC. When this occurs, the absorption due to the $\pi-\pi^*$ band decreases and that due to the n$-\pi^*$ band increases. The excitation of the n$-\pi^*$ transition of *cis*-AzoLC at around 450 nm results in a transformation to *trans*-AzoLC with an increase in the $\pi-\pi^*$ band and a decrease in the n$-\pi^*$ band. These phenomena are typical of azo derivatives. In the initial state, the AzoLC is in the trans form. This has a rodlike shape and stabilizes the structure of the nematic phase, because it is similar to 5CB. On the other hand, the photoinduced cis form has a bent shape and hence tends to disorganize the nematic phase structure and induce a nematic−isotropic isothermal phase transition. These results indicate that the optical properties could be switched completely by light irradiation. It was confirmed that these changes could be reversed over six cycles by alternate irradiation with UV and visible light.

Mechanism of the Change in the Optical Properties. The effective refractive indices of LCs were evaluated to obtain information about the orientation of the LCs in the voids in the inverse opal films and to investigate the mechanism of the change in the optical properties. The optical properties of the opal and the inverse opal structures can be calculated using Maxwell's equation. As an approximation, the wavelength of the reflection peak can be calculated using the equation for Bragg diffraction under normal incidence:[7]

$$\lambda = 2\sqrt{\frac{2}{3}}d(n_{\text{silica}}{}^2 f + n_{\text{void}}{}^2 (1-f))^{1/2}$$

where λ is the peak position, d is the diameter of the spherical voids, n_{silica} and n_{void} are the refractive indices of the SiO_2 and the medium in the voids of the inverse opal films, respectively, and f is the volume fraction of SiO_2.

For the evaluation of the effective refractive indices of the LCs (n_{LCeff}), the parameters d and f of the inverse opal films were determined by plotting their peak positions against the refractive indices using several solvents with different refractive indices: methanol ($n = 1.329$), ethanol ($n = 1.360$), toluene ($n = 1.496$), and 1,2-dibromoethane ($n = 1.538$). The relationship between the refractive indices and the peak positions is shown in the Supporting Information. By fitting the equation to the experimental measurements with the fixed constant value $n_{\text{silica}} = 1.45$, the values of d and f were determined as 239 and 0.131, respectively.

Figure 4 shows the variation of n_{LCeff} with temperature, which was calculated from the equation using the parameters determined above. The true value of the refractive index of 5CB (n_{LC}) was also measured using an Abbe refractometer. The change in n_{LCeff} was similar to that in n_{LC} without the inverse opal structure. In the isotropic phase, both of the values are the same. In the nematic phase, the changes in value also behaved in the same way, although the values in the inverse opal films were a little closer to the average. These results suggested that the two peaks observed in the reflection spectra were derived from n_{LC}, and the shorter wavelength peak and the longer wavelength peak correspond to n_o (ordinary refractive index) and n_e (extraordinary refractive index), respectively. It can be assumed that the LCs in the nematic phase in the voids of the inverse opal are aligned parallel to the void surfaces, forming

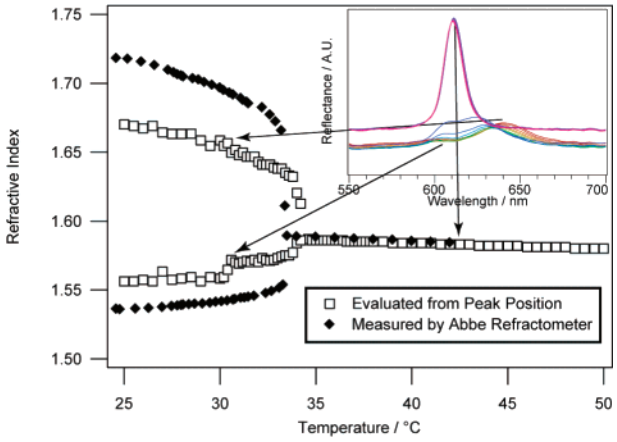

Figure 4. Refractive indices: evaluated from Bragg's equation, ◆; measured by an Abbe refractometer, □.

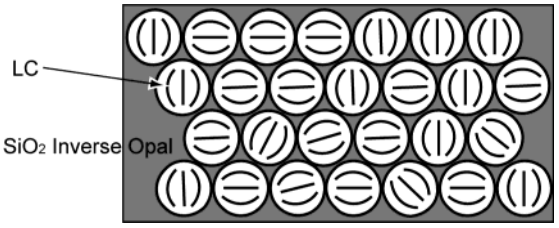

Figure 5. Model of the orientation of liquid crystals in the voids in inverse opal film. The lines in the circles represent the orientation of the LCs.

the well-known bipolar structure,[55−57] and that the orientation of the polar axes of the bipolar structure of the LCs in the different voids is random overall, as shown in Figure 5. The two peaks can be attributed to diffractions from domains existing in different places in the films. The peak corresponding to n_o would be observed from domains where the axes are parallel to the incident light, and the peak corresponding to n_e would be observed from those domains where the axes are perpendicular to the incident light. However, most of the light was scattered and the peaks were weakened because such a random structure does not satisfy the conditions required for Bragg diffraction. On the other hand, when the LCs were transformed into the isotropic phase, the optical anisotropy disappeared, and the reflection peak due to Bragg diffraction appeared.

Separation and Control of the Two Peaks. According to the mechanism we proposed above, the two peaks in the nematic phase can be separated and controlled by the alignment of the LCs. If all of the axes of the bipolar structure of the LCs are aligned parallel to the glass substrate, the incident light will encounter both n_e and n_o, and the two corresponding peaks will be observed. Similarly, when all of the axes are aligned perpendicular to the glass substrate, the incident light will only encounter n_o, and one corresponding peak will be observed at shorter wavelength (Figure 6). Two samples were prepared, on the basis of this premise. The inverse opal films were covered with other pieces of glass, which were coated with an alignment layer consisting of polyimide compounds, and which can induce homogeneous alignment (sample A) or homeotropic alignment (sample B). The voids in the film were filled with the same LC (5CB). It can be expected that the alignment layer will affect

(55) Springer, G. H.; Higgins, D. A. *J. Am. Chem. Soc.* **2000**, *122*, 6801.
(56) Luther, B. J.; Springer, G. H.; Higgins, D. A. *Chem. Mater.* **2001**, *13*, 2281.
(57) Rudhardt, D.; Fernández-Nieves, A.; Link, D. R.; Witz, D. A. *Appl. Phys. Lett.* **2003**, *82*, 2610.

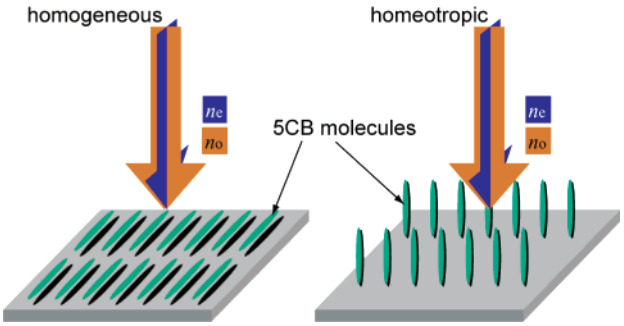

Figure 6. Model of the refractive indices encountered by the incident light in the cases of homogeneous alignment (left), and homeotropic alignment (right).

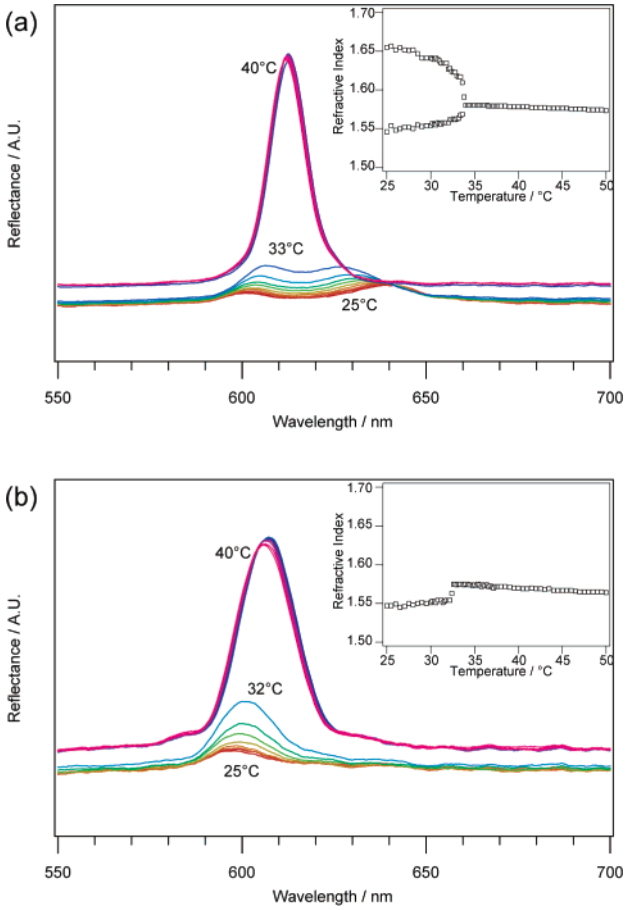

Figure 7. Reflection spectra of 5CB-infiltrated inverse opal films that were covered with an alignment layer-coated glass substrate: (a) homogeneous alignment, (b) homeotropic alignment. The spectra are plotted for temperature increments of 1 °C. The changes in the effective refractive indices evaluated from the peak positions are shown in the inset.

the orientation of LCs near to it and that this orientation will spread to the other LCs in the spherical voids in the inverse opal via the holes that connect each of the voids, although the effect will not extend over the whole film. Figure 7 shows the reflection spectra of samples A and B. Two peaks corresponding to n_e and n_o can be observed in the spectrum of sample A. On the other hand, only one peak corresponding to n_o can be observed in the spectrum of sample B. The changes in the effective refractive indices evaluated from the peak positions behaved in the same way as those of n_e and n_o of 5CB (Figure 7, inset). These results agree with the expectations described above. Furthermore, we succeeded in the separation of the two

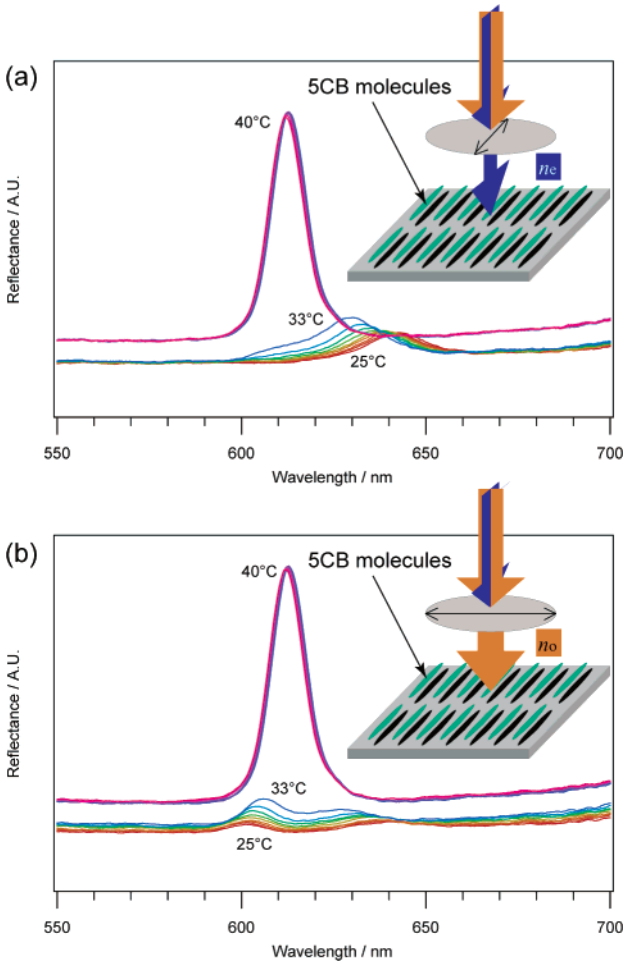

Figure 8. Reflection spectra of 5CB-infiltrated inverse opal films that were covered with an alignment layer-coated glass substrate. The measurements were performed with the polarizer set parallel to the alignment direction (a), and perpendicular to the alignment direction (b). The spectra are plotted for temperature increments of 1 °C. The insets are the model of the refractive indices encountered by the incident light through the polarizer.

peaks in sample A by using linearly polarized incident light that was passed through a polarizer. As shown in Figure 8, the peak corresponding to n_e could be observed when the plane of the polarized light was parallel to the axes of the LCs, and that corresponding to n_o could be observed when the plane was perpendicular to the axes. Such a separation can be explained by the mechanism shown in the inset of Figure 8. When the plane of the polarized light is parallel to the axes of the LCs, n_e will be dominant, and when it is perpendicular, n_o will be dominant. These results are consistent with the theoretical analysis. Some research groups have reported that the anisotropy causes the disappearance of the degeneracy of the photonic band, leading to nondegenerate band gaps. Therefore, separate reflection peaks can be observed, and each of the peaks will reflect incident light that has one of the two polarizations.[47,58−60] This agrees with our experiments using sample A. On the other hand, when sample B was used, the axes of the LCs are parallel to the incident light, and there is no anisotropy. That is why only one peak could be observed.

These results showed that the optical properties could be controlled by changing the alignment of the axes. They also

(58) Li, Z.-Y.; Wang, J.; Gu, B.-Y. *Phys. Rev. B* **1998**, *58*, 3721.
(59) Li, Z.-Y.; Lin, L.-L.; Gu, B.-Y.; Yang, G.-Z. *Physica B* **2000**, *279*, 159.
(60) Zabel, I. H. H.; Stroud, D. *Phys. Rev. B* **1993**, *48*, 5004.

show that the two peaks correspond to n_e and n_o and support the assumption that the LCs formed a bipolar structure in each of the voids in the inverse opal film. The reason the values for n_{LCeff} do not agree with those for n_{LC} can also be explained by the bipolar structure. In such an alignment, some molecules are slanted toward the axes of the domain, leading to refractive indices that are closer to the average value. It should be noted that, for all considerations described above, we assumed that the LCs were only infiltrated into the spherical voids in the inverse opal structure. In fact, there is a possibility that LCs are also infiltrated into the SiO_2 frameworks because the SiO_2 framework may be porous, as indicated by the lower value for the volume fraction of SiO_2 than would be expected for a perfect FCC structure. If this is the case, the LCs in the framework should have completely random orientations. This would lead to light scattering, but would not have a serious effect on optical properties such as the optical stop band. Therefore, the interpretation described above should still be valid even if LCs are infiltrated into the SiO_2 framework.

The same phenomena were observed when 6CB, 7CB, and 8CB were used. They showed drastic changes in their optical properties at the phase transition temperature. Separation of the two peaks could be realized, and the behavior of the effective refractive indices was similar to that of the respective LCs without the inverse opal structure. These results are shown in the Supporting Information.

It was also confirmed that control of the optical properties could be realized by using a system of photoinduced phase transitions. An inverse opal film with an alignment layer that can induce homogeneous alignment was prepared, and a mixture of 5CB and AzoLC was infiltrated. Figure 9a shows the change in the reflection spectra of this sample by light irradiation. The spectra are shown at 2-s steps during the irradiation. Two peaks could be observed in the initial state, while a distinct single peak appeared at the phase transition. Additionally, these two peaks could be controlled by the use of a polarizer. Figure 9b shows the reflection spectra measured with linearly polarized light. When the plane of the polarized light was parallel to the axes of the LCs, a peak at around 640 nm and a weak peak at around 600 nm could be observed. On the other hand, when the plane of the polarized light was perpendicular to the axes of the LCs, the former peak became weaker and the latter peak became stronger. These results are in good agreement with those observed for the control of the temperature.

Conclusions

We have succeeded in fabricating an LC-infiltrated inverse opal structure. The structure showed optical properties quite different from those of an inverse opal structure without the LCs. Control of the optical properties was realized by thermal and photoinduced isothermal phase transitions. We have also succeeded in elucidating both the orientation of the LCs and the mechanism of the switching of the optical properties by the evaluation of the effective refractive indices. Furthermore, it was found that a change in the optical properties could also be realized by controlling the alignment axes of the LCs in each of the voids in the inverse opal film. This gives the basis of a technique for controlling the optical properties by the use of external stimuli. Additionally, these results will provide useful information for studies into the states of LCs in restricted spaces.

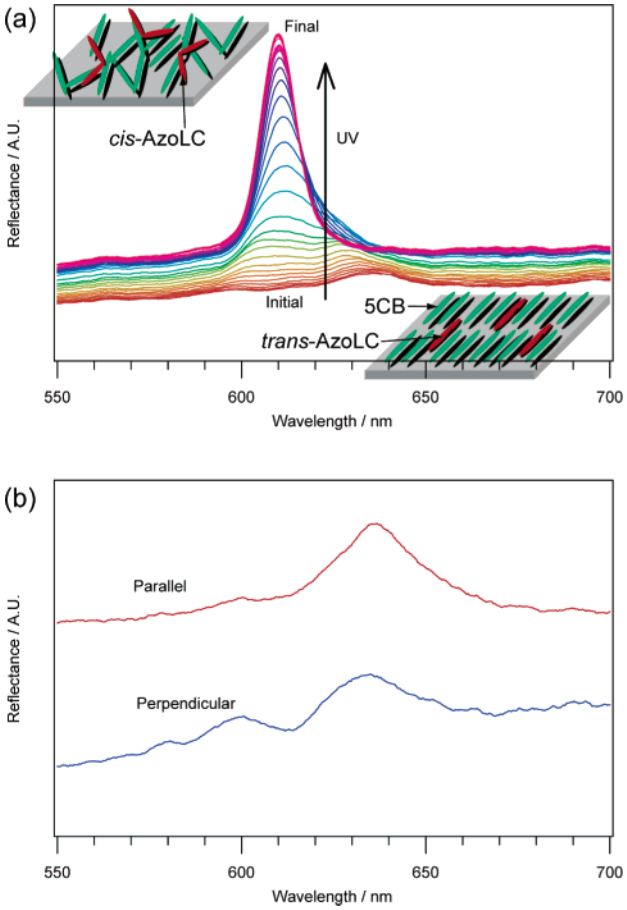

Figure 9. (a) Reflection spectra of a mixture of 5CB and AzoLC-infiltrated inverse opal films covered with an alignment layer. (b) Reflection spectra in the initial state measured wit linearly polarized incident light. The insets of (a) show the model of orientation before and after irradiation with UV light.

They suggest that the inverse opal structure has the potential to provide a system for investigating the states of LCs by considering the optical properties of a photonic band gap material.

It can be expected that these results will contribute to studies of the detailed properties of liquid crystals and also to the realization of tunable photonic band gap materials with large changes in their optical properties.

Acknowledgment. We are indebted to Prof. T. Ikeda, Dr. O. Tsutsumi, and Dr. A. Shishido for measuring the refractive indices of LCs by means of an Abbe refractometer. We are also grateful to Prof. T. Kato and Mr. K. Yabuuchi for instructions in parts of our experiments. This work was supported by a Grant-in-Aid for Scientific Research on Priority Areas (417) from the Ministry of Education, Culture, Sports, Science, and Technology (MEXT) of the Japanese Government. This work was also supported by Research Fellowships of the Japan Society for the Promotion of Science on Young Scientists.

Supporting Information Available: The relationship between the refractive indices of the media in the voids in the inverse opal and the peak positions. Also shown are the changes in the optical properties of LCs-infiltrated inverse opal films when 6CB, 7CB, and 8CB were used. This material is available free of charge via the Internet at http://pubs.acs.org.

JA0495056